The Evolution of Antimicrobial effectiveness of Nano-AgO particles against various Pathogens such as *Pseudomonas aeruginosa* and *Streptococcus pyogenes*, synthesized and characterized through the Chemical Reduction Method

Gundala Madan Kumar[1], Ginne Kalpana[3], Ravinder M.[2] and Shanmukha Kumar J.V.[1]*
1. Department of Chemistry, Koneru Lakshmaiah Education Foundation, Guntur, Andhra Pradesh, INDIA
2. Department of Chemistry, Chaitanya (Deemed to be University), Hanamakonda, Warangal, Telangana, INDIA
3. Vaagdevi Engineering College, Bollikunta, Warangal, Telangana State, INDIA
*shanmukhakumar.klu@gmail.com

Abstract
This investigation focused on the production of nano-AgO particles using the traditional chemical reduction method. The nano-AgO particles forged in the lab show a fierce ability to take down bacteria and their increased reactivity is born from a mighty surface-to-volume ratio. The crafted nano-AgO particles underwent rigorous inspection using a range of methods including Transmission Electron Microscopy (TEM), Scanning Electron Microscopy (SEM), Fourier Transform Infrared Spectroscopy (FTIR) and X-ray Diffraction Spectroscopy (XRD).

The results showed that the nano-AgO particles were made up of clusters of smaller bits, mostly measuring between 100 and 200 nm in size. The trials demonstrated that the nano-AgO particles were highly effective at eliminating bacteria including P. aeruginosa and S. pyogenes, resulting in a 17 mm stretch free from any growth.

Keywords: Synthesis of nano-AgO particles, Chemical reduction (CR), Antimicrobial activity, TEM, SEM, FTIR and XRD.

Introduction

During challenging times, maintaining safety and cleanliness became essential due to low yields, complex purification processes and the significant energy consumption associated with chemical reductions. The exact mechanism by which those nano-AgO particles eliminate troublesome bacteria, remains unclear. Nanotechnology is a new frontier that has recently caused quite a stir in the scientific community. We are examining particles ranging from 1 to 100 nm under a microscope. Nano-AgO particles stand out in the field of metallic nanoparticles because of their unique physical, biological and chemical properties[3].

It is important to note that converting silver ions into metal nano-AgO particles through an appropriate chemical reduction method reduces toxicity while greatly enhancing antibacterial properties[5]. Metal nanoparticles produced via chemical processes have established their roles in antimicrobials, healing remedies, biomolecule detection and catalysis, among many other applications. It is said that silver NPs, as small as a rattlesnake's fang under 200 nm in size, offer significant advantages[2,12]. Their appeal lies in their highly reactive surface, which facilitates optimal interaction with the environment[7]. Many studies have shown the pathogen-fighting power of those positively charged species. A variety of bottom-up methods, such as chemical reduction, can generate some nano-AgO particles.

We often use fast and reliable methods of chemical reduction[18]. By handling sodium borohydride and other trusted reducing agents, one can lower the concentration to an optimal level[14]. The chemical reduction process, well known for producing nanoparticles, employs an organic solvent such as ethylene glycol[17], along with reliable reducing agents like hydrazine[11], sodium borohydride[15], trisodium citrate[10] and ascorbate[9]. This process also involves the use of a highly effective reducing agent. The formation of nanoparticles associated with these processes depends on their attraction to negatively charged bacterial cells[4,13]. This study aims to investigate the antibacterial potential of CR-synthesized nano-AgO particles against various Gram-negative and Gram-positive bacteria including *P. aeruginosa* and *S. pyogenes*, using antimicrobial testing as a reliable guide.

Material and Methods

Materials: 98% pure $Ag(NO_3)_2$, 98% pure $NaBH_4$, 98% pure sodium alginate, 98% pure THF and 99% pure deionized water were exclusively supplied by S.D. Fine Chemicals.

Nano-AgO Particles Synthesis: We used CR to synthesize nano-AgO[16]. First, we mixed 0.1 M $Ag(NO_3)_2$ with 100 mL of deionized water to prepare nano-AgO particles. Then, we dissolved 0.1 M $NaBH_4$ in 100 mL of THF. We also prepared a 10% sodium alginate solution by mixing 100 mL of sodium alginate into deionized water. Next, we poured 50 mL of the 0.1 M $Ag(NO_3)_2$ solution into a flask. This was stirred vigorously with a magnetic stirrer at 60–70°C for 1 hour, regardless of the reaction's heat or cooling time. Afterwards, 40 mL of the $NaBH_4$ solution was gradually added, followed by 25 mL of the sodium alginate solution, stirred continuously for 10–15 minutes. Finally, the mixture was

gently stirred at 50–60°C for 120 minutes until the nano-AgO precipitate, changing from light yellow to dusty brown.

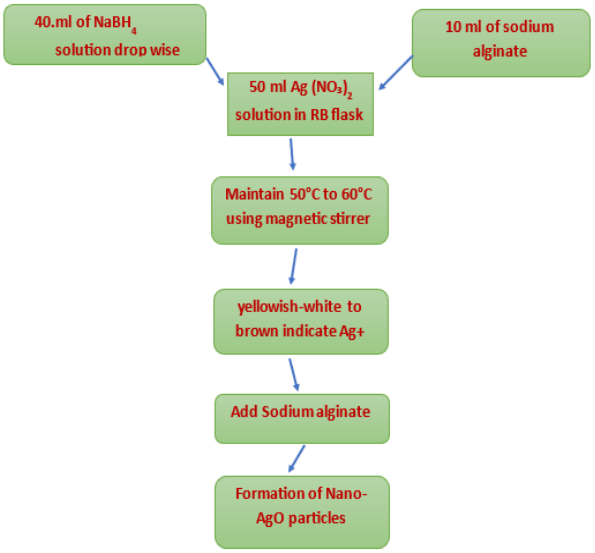

Results and Discussion

Transmission Electron Microscopy (TEM): Upon closely examining the CR reaction method, we discovered some impressive colloidal nano-AgO particles, as small as a rattlesnake's fang. The CR method, with the help of TEM images, shows that the nano-AgO particles are clearly shaped, small round particles that do not tend to stick together much. Using ImageJ software and transmission electron microscopy, we estimate that the nano-AgO particles have a diameter of about 200 nm, as shown in figs. 1 and 2. Besides the usual imaging, TEM can also detect changes in chemical composition, crystal orientation, electron structure and shifts in electron phase caused by the sample, using various modes. The details in figs. 3 and 4 reveal that those nano-AgO particles are both round and cubic, with a mixed structure and measure around 200 nm on average. Previous studies support this finding[6]. The CR method was found to influence particle size reduction directly.

Scanning Electron Microscopy (SEM): The study demonstrated that increasing the temperature from 50°C to 60°C leads to a significant decrease in particle size[8]. Figs. 5 and 6 present high-resolution SEM images showing precipitates next to a dusting of nanoscale AgO particles. The observation of nano-AgO particles indicates their tendency to cluster, resulting in larger particles that may suggest the presence of these NPs. The high-quality SEM images obtained via the CR method are due to a large surface area and high surface energy. The study found that the crystalline nano-AgO particles typically measure between 100 and 200 nm. The variation in size aligns with the diverse surface morphologies of the nano-AgO particles. Fig. 7 shows that the surface of these particles features a finely detailed structure, with granules approximately 100 to 200 nm in size as seen in fig. 8.

X-Ray Diffraction (XRD): A comprehensive analysis was conducted to identify the crystalline features of nano-AgO particles produced by the CR method using $Ag(NO_3)_2$. Fig. 9 presents a detailed XRD pattern illustrating the characteristics of CR-synthesized AgO nanoparticles.

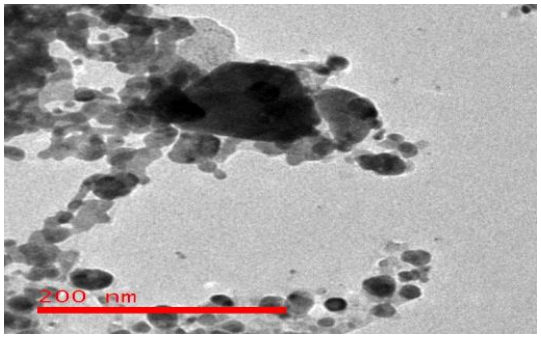

Figure 1

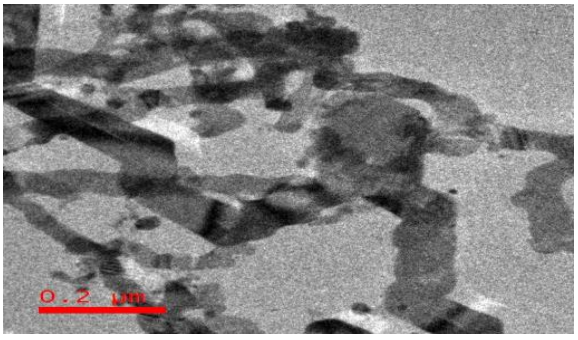

Figure 2

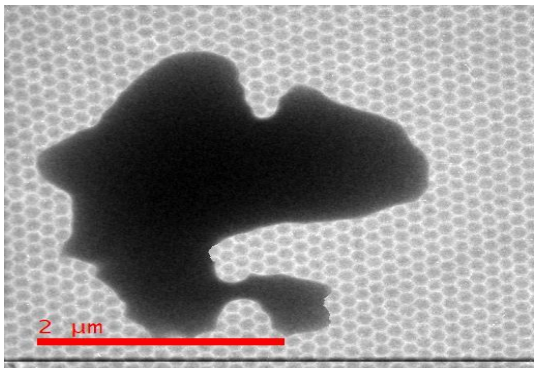

Figure 3

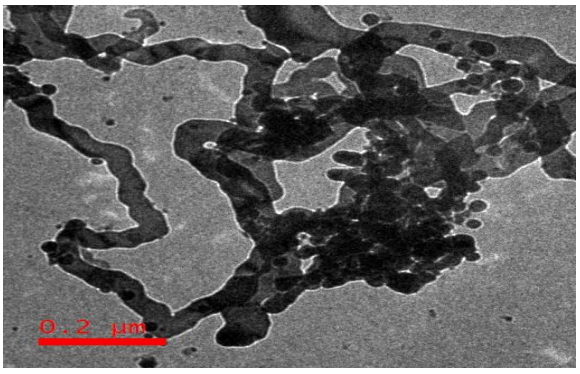

Figure 4

Figs. 1, 2, 3 and 4: TEM-Images of Nano-AgO particles

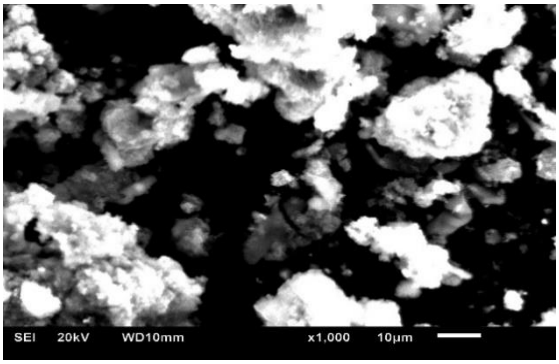

Figure 5

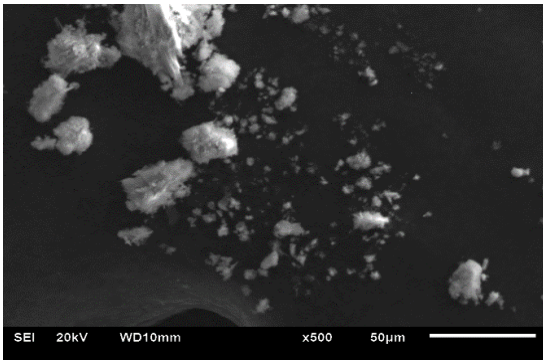

Figure 6

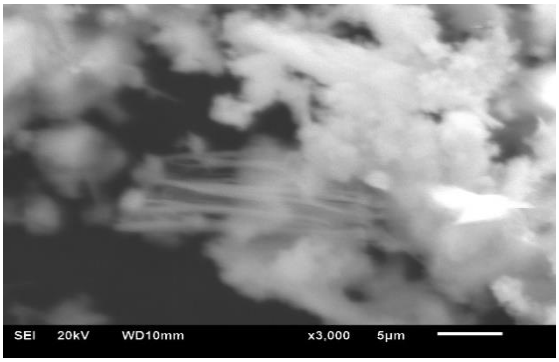

Figure 7

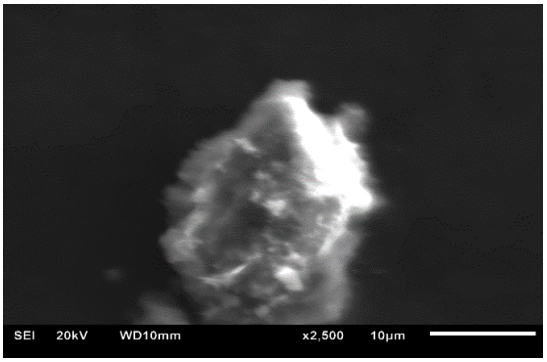

Figure 8

Figs. 5, 6, 7 and 8: SEM-Images of Nano-AgO particles

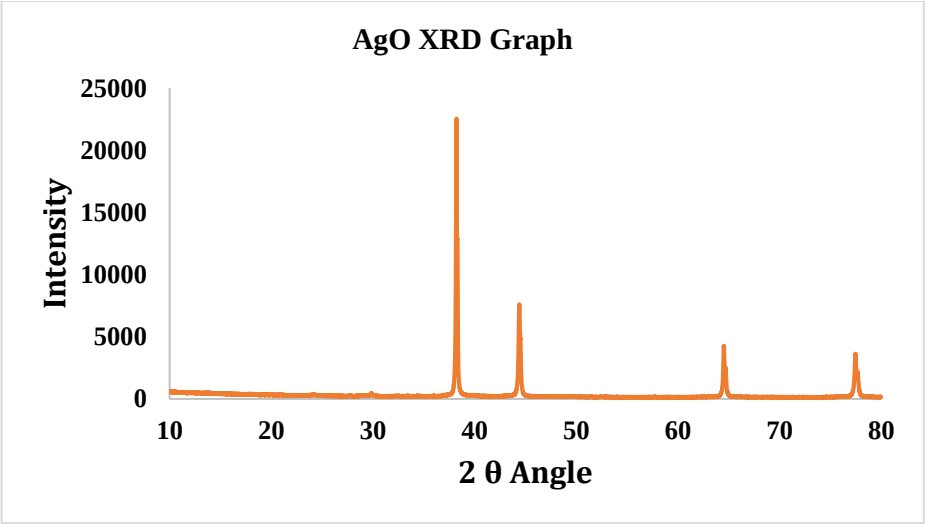

Figure 9: X-ray Diffraction graph of Nano-AgO particles

Four distinct peaks appear at 2θ values of 38.2°, 44.1°, 64.1° and 77.0°, corresponding to the (111), (200), (220) and (311) planes respectively. The average size of these nano-AgO particles, calculated via the Debye-Scherrer equation, is approximately 200 nm. The nanocrystalline nature of AgO facilitates the identification of differences in diffraction peaks.

As shown in fig. 9, the samples display a transformation into single crystals with AgO particles predominantly aligned along the (111) and (200) directions. The eco-friendly CuO NPs exhibit similar diffraction peaks and crystalline features, consistent with previous accounts[1]. The diffraction pattern of a reference nano-AgO sample shows two broad peaks at 38.2° and 44.1°, indicating a face-centered cubic crystalline structure.

FTIR (Fourier Transform Infrared) Spectroscopy: We conducted FTIR studies to evaluate the stability and composition of the synthesized nano-AgO particles. Fig. 10 reveals a shoulder peak at 1660.42 cm^{-1} and a prominent band at 2359.94 cm^{-1}, confirming the presence of nano-AgO particles. The O-H bending vibration of adsorbed water appears at 3424.78 cm^{-1}, indicating surface moisture. A notable band at 2925.76 cm^{-1} suggests the stretching vibration of C=O, likely due to water vapor and atmospheric

CO_2. The absorption band at 1384.11 cm^{-1} signifies NO_2, associated with the nitronium ion alongside $Ag(NO_3)_2$. A C-C single bond stretching vibration is observed at 1274.84 cm^{-1}, characteristic of the solvent. Peaks between 917.61 cm^{-1} and 717.94 cm^{-1} indicate slight C-H bending vibrations, while weaker O-H bending vibrations are seen between 669.98 cm^{-1} and 457.17 cm^{-1}. Overall, the FTIR analysis confirms the successful synthesis and potential of the nano-AgO particles.

Anti-Microbial Activity: The broth dilution method was used to assess the antibacterial effectiveness of nano-AgO particles against both Gram-negative and Gram-positive bacteria including *P. aeruginosa* and *S. pyogenes*. The results show that nano-AgO particles are highly effective in killing Gram-negative bacteria. After the addition of 10^7 CFU into 1 ml of the final inoculum, which contained 108 CFU bacteria, equal amounts of each sample were added. The broth components were dissolved in distilled water before being transferred into sterile microtubes.

Mueller-Hinton broth (MHB) was used as the medium for culturing *P. aeruginosa* and *S. pyogenes* for 24 hours at 37°C, with stirring at 200 rpm. Subsequently, we prepared multi-concentration solutions of nano-AgO using distilled water. The molecular weights are as follows: 0.0012, 0.0024, 0.0037, 0.0049, 0.0061, 0.0074, 0.0086, 0.0096, 0.0111 and 0.0123. The concentrations were precisely prepared in mg at intervals of 10, 20, 30, 40, 50, 60, 70, 80, 90 and 100.

On MHB agar Petri plates, two bacterial strains were exposed to different concentrations of nano-silver oxide solutions. A reaction mixture without nano-AgO particles was prepared in the MHB plate well, following the same conditions as the control. Before measuring the inhibitory zone, two MHB Petri plates are incubated at 37°C for 24 hours. The recorded measurements of the inhibitory zones for *P. aeruginosa* were 1.5, 2.8, 4.3, 7.2, 9.8, 12, 15.5, 17.2, 20.5 and 22 mm, corresponding to concentrations of 10, 20, 30, 40, 50, 60, 70, 80 and 90 mg.

The values of the inhibition zone for *S. pyogenes* start at 10 mg, with measurements documented at 1.0, 4.5, 7.5, 9.7, 11.5, 13.4, 15.2, 17, 18.3 and 11 mm, each corresponding to the respective concentrations of the nano-AgO solution. The results demonstrate that *P. aeruginosa* is most susceptible to the strong antibacterial properties of nano-AgO particles, as shown in figs. 11 and 12. At the exact dosage of AgO NPs, it is clear that Gram-negative bacteria such as *P. aeruginosa* exhibit a more pronounced zone of inhibition compared to Gram-positive bacteria like *S. pyogenes* and *Klebsiella*, with relevant values detailed in table 1. Figs. 13 (a, b, c) and 14 (a, b, c) display the zone of inhibition for *P. aeruginosa* and *S. pyogenes*.

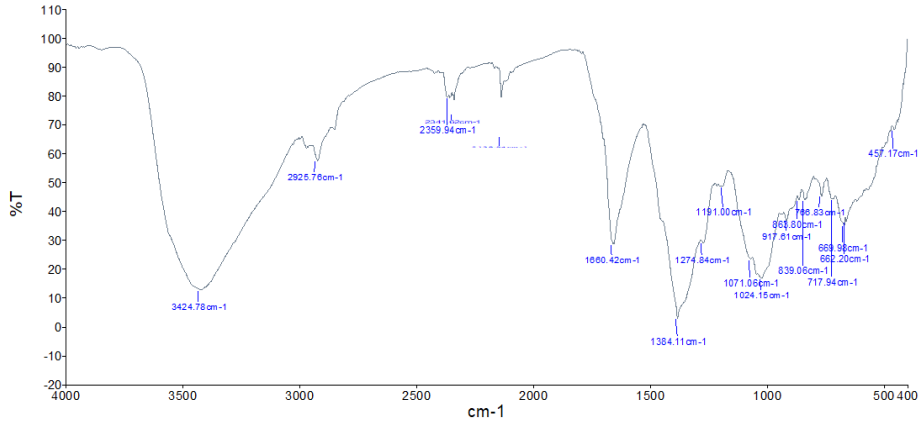

Figure 10: FTIR Graph of Nano-AgO particles

Table 1
Zone of inhibition standards of Anti-Microbial activity

S.N.	Conc. of Nano-AgO		Zone of inhibition in mm	
	In Moles	In mg	*P. aeruginosa*	*S. Pyogenes*
1.	0.0012	10	1.5	1.0
2.	0.0024	20	2.8	4.5
3.	0.0037	30	4.3	7.5
4.	0.0049	40	7.2	9.7
5.	0.0061	50	9.8	11.5
6.	0.0074	60	12	13.4
7.	0.0086	70	15.5	15.2
8.	0.0096	80	17.2	17
9.	0.0111	90	20.5	18.3
10.	0.0123	100	22	19

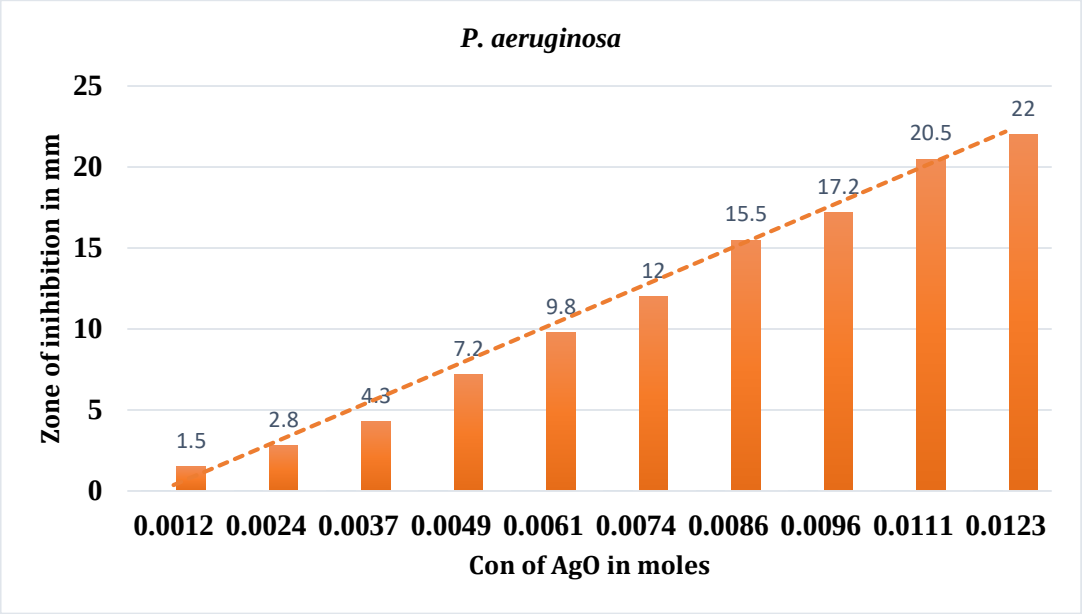

Figure 11: Graph of Anti-Microbial activity of nano-AgO with *P. Aeruginosa*

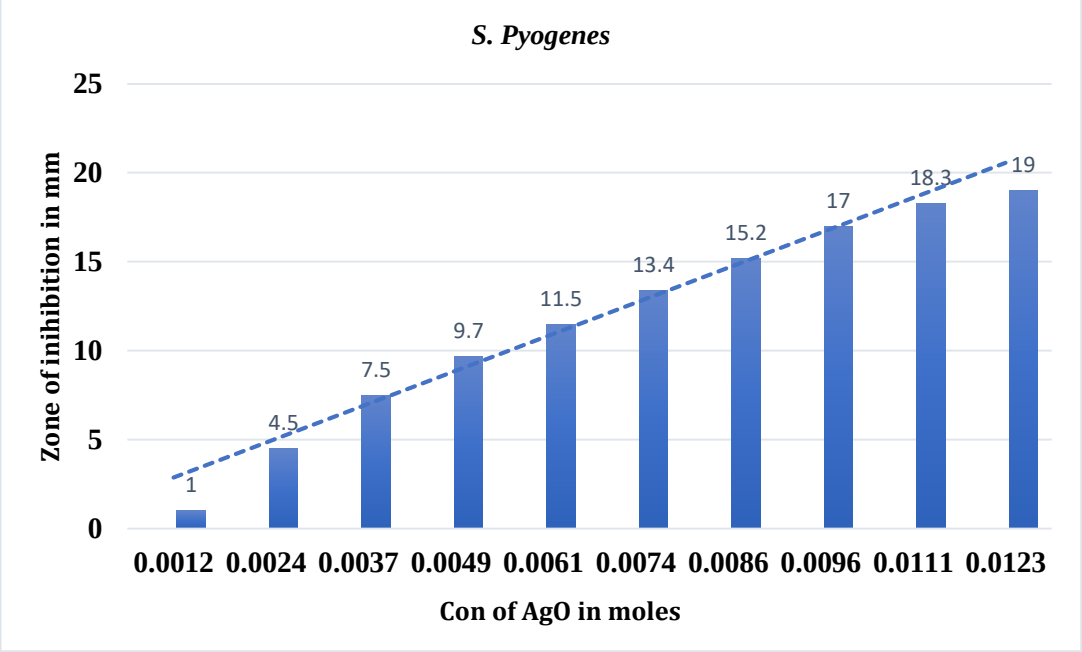

Figure 12: Graph of Anti-Microbial activity of Nano-AgO with *S. Pyogenes*

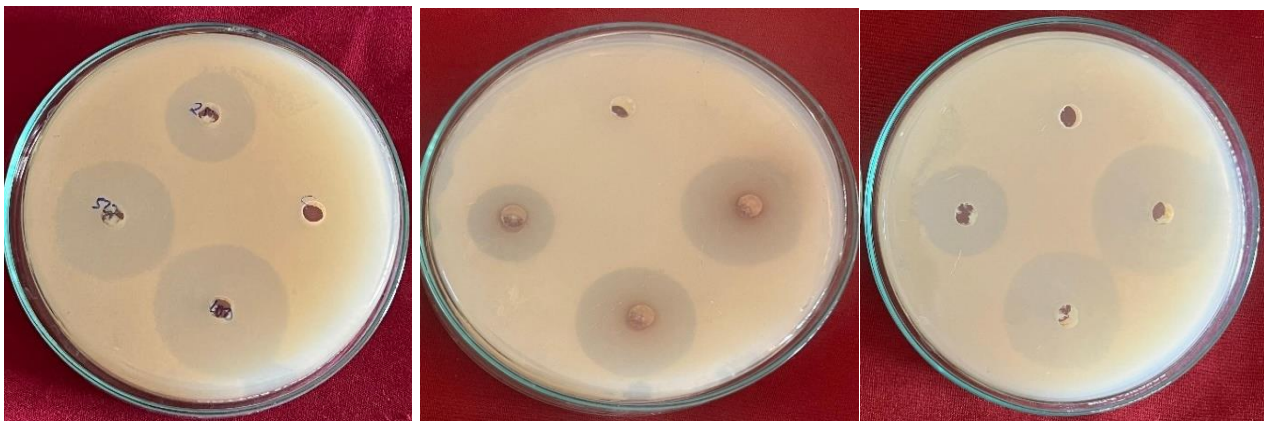

(a) **(b)** **(c)**

Figure 13 (a), (b) and (c): Zone of inhibition for *P. Aeruginosa* with AgO NPs

(a) **(b)** **(c)**

Figure 14 (a), (b) and (c): Zone of inhibition for *S. Pyogenes* with AgO NPs

Conclusion

We presented a straightforward method for synthesizing nanoscale AgO particles from an aqueous $Ag(NO_3)_2$ solution. TEM and SEM images confirmed the presence of nano-AgO particles smaller than 200 nm. The synthesis of spherical, face-centered and cubic nano-AgO particles was validated through XRD and FTIR analysis. The broth dilution technique was used to assess the effectiveness of nano-AgO particle dispersion in inhibiting bacterial growth. This study showed that colloidal nano-AgO particles prevented the growth and reproduction of both Gram-negative and Gram-positive bacteria, specifically *Pseudomonas aeruginosa* and *Streptococcus pyogenes*.

Combining Nano-AgO particles with antibiotics offers a promising approach to combat drug-resistant bacteria. This suggests that nano-AgO particles could be potential treatments for urinary tract infections, pneumonia, intra-abdominal infections, bloodstream infections, scarlet fever and sepsis, especially in cases involving multidrug-resistant bacteria.

References

1. Apriandanu D.O.B. and Yulizar Y., Tinospora crispa leaves extract for the simple preparation method of CuO nanoparticles and its characterization, *Nano-Struct. Nano-Objects*, **20**, 100401 **(2019)**

2. Christopher P., Xin H. and Linic. S., Visible-light-enhanced catalytic oxidation reactions on plasmonic silver nanostructures, *Nat. Chem*, **3(6)**, 467-472 **(2011)**

3. Franci, G., Falanga, A., Galdiero S., Palomba L., Rai M. and Morelli G., Silver Nanoparticles as Potential Antibacterial Agents, *Molecules*, **20**, 8856–8874 **(2015)**

4. Hamouda T. and Baker Jr., Antimicrobial mechanism of action of surfactant lipid preparations in enteric Gram-negative bacilli, *J. Appl. Microbiol*, **89**, 397-403 **(2000)**

5. Jadhav K., Dhamecha D., Bhattacharya D. and Patil M., Green and eco-friendly synthesis of silver nanoparticles: Characterization, biocompatibility studies and gel formulation for treatment of infections in burns, *J. Photochem. Photobiol.*, **155**, 109–115 **(2016)**

6. Jangir L.K. et al, Investigation of luminescence and structural properties of ZnO nanoparticles, synthesized with different precursors, *Chem. Front*, **1**, 1413–1421 **(2017)**

7. Krutyakov Y.A.., Kudrinskiy A.A., Olenin A.Y. and Lisichkin G.V., Synthesis and properties of silver nanoparticles: advances and prospects, *Russian Chem Re*, **77**, 233-257 **(2008)**

8. Lu C.H. and Yeh C.H., Influence of hydrothermal conditions on the morphology and particle size of zinc oxide powder, *Ceram. Int*, **26**, 351–357 **(2000)**

9. Qin Y., Ji X., Jing J., Liu H., Wu H. and Yang W., Size control over spherical silver nanoparticles by ascorbic acid reduction, *Colloids Surf a Physicochem Eng. Asp*, **372(1-3)**, 172-176 **(2010)**

10. Rashid M.U., Bhuiyan M.K.H. and Quayum M.E., Synthesis of Silver Nano Particles (Ag-NPs) and their uses for Quantitative Analysis of Vitamin C Tablets, *J Pharm Sci*, **12(1)**, 29–33 **(2013)**

11. Roshmi T. et al, Antibacterial properties of silver nanoparticles synthesized by marine *Ochrobactrum* sp, *Braz. J. Microbiol*, **45(4)**, 1221-1227 **(2014)**

12. Sadhasivam S., Shanmugam P. and Yun K., Biosynthesis of silver nanoparticles by Streptomyces hygroscopicus and antimicrobial activity against medically important pathogenic microorganisms, *Colloids Surf Biointerfaces*, **81(1)**, 358-62 **(2010)**

13. Sagar Milind, Pandey Prashant Kumar, Jyothi MS, Sharma Shiva and Rastogi Manisha, Evaluation of in vitro anticancer efficacy of Eleaocarpus ganitrus (Rudraksha) bead derived silver nanoparticles, *Res. J. Biotech.*, **19(9)**, 28-35 **(2024)**

14. Sondi I. and Salopek-Sondi B., Antimicrobial mechanism of action of surfactant lipid preparations in enteric Gram-negative bacilli, *Interface. Sci*, **275(4)**, 177-82 **(2004)**

15. Song K.C., Lee S.M. and Park T.S., Preparation of colloidal silver nanoparticles by chemical reduction method, *Korean J Chem Eng*., **26(1)**, 153–5 **(2009)**

16. Wang L. and Muhammed M., Synthesis of zinc oxide nanoparticles with controlled morphology, *J. Mater. Chem*, **9**, 2871-2878 **(1999)**

17. Wiley B., Herricks T., Sun Y. and Xia Y., Polyol Synthesis of Silver Nanoparticles: Use of Chloride and Oxygen to Promote the Formation of Single-Crystal, Truncated Cubes and Tetrahedrons, *Nano Lett*, **4(9)**, 1733–1739 **(2004)**

18. Zielin´ska A., Skwarek E., Zaleska A., Gazda M. and Hupka J., Preparation of silver nanoparticles with controlled particle size, *Procedia Chemistry*, **1(2)**, 1560–1566 **(2009)**.

(Received 13th August 2025, accepted 06th October 2025)